



# Synthesis of acid–base bifunctional mesoporous materials by oxidation and thermolysis

Xiaofang Yu <sup>a</sup>, Yongcun Zou <sup>b</sup>, Shujie Wu <sup>a</sup>, Heng Liu <sup>a</sup>, Jingqi Guan <sup>a,\*</sup>, Qiubin Kan <sup>a,\*</sup>

<sup>a</sup> College of Chemistry, Jilin University, Jiefang Road 2519, Changchun 130023, PR China

<sup>b</sup> State Key Laboratory of Inorganic Synthesis and Preparative Chemistry, College of Chemistry, Jilin University, Changchun 130012, PR China

## ARTICLE INFO

### Article history:

Received 29 September 2010

Received in revised form 23 December 2010

Accepted 12 February 2011

Available online 18 February 2011

### Keywords:

- A. Structural materials
- B. Chemical synthesis
- C. X-ray diffraction
- D. Catalytic properties

## ABSTRACT

A novel and efficient method has been developed for the synthesis of acid–base bifunctional catalyst  $\text{SO}_3\text{H-MCM-41-NH}_2$ . This method was achieved by co-condensation of tetraethylorthosilicate (TEOS), 3-mercaptopropyltrimethoxysilane (MPTMS) and (3-triethoxysilylpropyl) carbamic acid-1-methylcyclohexylester (3TAME) in the presence of cetyltrimethylammonium bromide (CTAB), followed by oxidation and then thermolysis to generate acidic site and basic site. X-ray diffraction (XRD) and transmission electron micrographs (TEM) show that the resultant materials keep mesoporous structure. Thermogravimetric analysis (TGA), X-ray photoelectron spectra (XPS), back titration, solid-state  $^{13}\text{C}$  CP/MAS NMR and solid-state  $^{29}\text{Si}$  MAS NMR confirm that the organosiloxanes were condensed as a part of the silica framework. The bifunctional sample ( $\text{SO}_3\text{H-MCM-41-NH}_2$ ) containing amine and sulfonic acids exhibits excellent acid–basic properties, which make it possess high activity in aldol condensation reaction between acetone and various aldehydes.

© 2011 Elsevier Ltd. All rights reserved.

## 1. Introduction

Since the discovery of ordered mesoporous silicates M41S was reported [1,2], surface-modified mesoporous structural materials have been extensively investigated in recent years for catalysis [3–5], separation [6,7] and sensor design [8]. Multifunctional catalytic materials play a pivotal role for achievement of highly efficient organic synthesis. Particularly nanomaterials with coexisting two antagonist functions, such as acid and base, are of great interest owing to their potential novel functions and a wide range of applications to various catalysis. These functionalities may be used to perform several steps in a reaction sequence or work in a cooperative manner to alter the characteristics of a single reaction, for example, rate, selectivity, and so forth [9–14].

The aldol condensation reaction is recognized as one of the most fundamental tools for the construction of new carbon–carbon bonds in the biochemical and purely chemical domains [15,16]. While aldol condensation has historically been catalyzed with homogeneous acids and bases, due to environmental and economic concerns, more current literature has focused on heterogeneous catalysts. It is demonstrated that heterogeneous catalysts are able to effectively catalyze condensation reaction through acid–base cooperative catalysis.

Generally, these heterogeneous catalysts are prepared by co-condensation or post-synthesis grafting [17–20]. In post-synthesis, organic functional groups are grafted through a reaction of a silane coupling agent with the free and geminal silanol groups on the surface of mesopores. However, the distribution of the functional groups on the surface of the pore wall is likely not uniform and the organic groups are grafted mainly on the external surface of the mesoporous particles or near the pore mouth due to the mass transfer limitation. Comparatively, the advantage of direct synthesis is that it produces materials with high loading and relatively uniform distribution of the functional groups. Davis and his coworkers reported bifunctional heterogeneous SBA-15 containing primary amine and sulfonic acid, phosphoric acid or carboxylic acid by co-condensation [12,13]. However, mesoporous materials functionalized with sulfonic acids and amines were unable to give rise to higher activities due to mutual destruction of stronger acids paired with amines in the one-pot synthetic process. What is more, these acid–base bifunctional mesoporous materials were prepared under acidic medium so that protonation of amino groups inevitably occurred. Therefore, interest in exploring some effective ways to avoid potential mutual destruction of antagonist functions and protonation of amino groups in the chemical synthesis process has been growing recently. Site isolation is an effective method to control the distance between functional groups. Our group has reported two acid–base bifunctional mesoporous materials Benzyl-APS-S-SBA-15 and Anthracyl-APS-S-SBA-15 by controlling steric hindrance [21]. Corriu et al. [22] and

\* Corresponding authors. Tel.: +86 431 88499140; fax: +86 431 88499140.  
E-mail addresses: [guanjq@jlu.edu.cn](mailto:guanjq@jlu.edu.cn) (J. Guan), [qkan@jlu.edu.cn](mailto:qkan@jlu.edu.cn) (Q. Kan).

Lu et al. [23] have also reported on bifunctionalized mesoporous materials containing an acidic site and a basic site isolated from one another.

In order to avoid potential mutual destruction of antagonist functions and protonation of amino groups, in this work, an alternative chemical synthesis route to the conventional method to prepare acid–base bifunctional materials was developed by co-condensation. These alternatives include oxidation of thiols to obtain the sulfonic acids and then thermolysis of carbamates to obtain the amines. The catalytic activity of acid–base bifunctional mesoporous materials has been investigated in aldol condensation reaction between acetone and various aldehydes.

## 2. Materials and methods

### 2.1. Materials

Cetyltrimethylammonium bromide (CTAB) (Aldrich), HCl (A.R.), H<sub>2</sub>O<sub>2</sub> (30%) (A.R.), tetraethyorthosilicate (Aldrich), 4-nitrobenzaldehyde (Acros), 4-(trifluoromethyl)benzaldehyde (Acros), 4-cyanobenzaldehyde (Acros), benzaldehyde (Acros), 1-methylcyclohexanol (Mch) (Acros), 3-(triethoxysilyl) propylisocyanate (TCI), 3-mercaptopropyltrimethoxysilane (MPTMS) (Acros), 3-aminopropyltriethoxysilane (APS) (Acros), and acetone (A.R.) were commercially available and used as received.

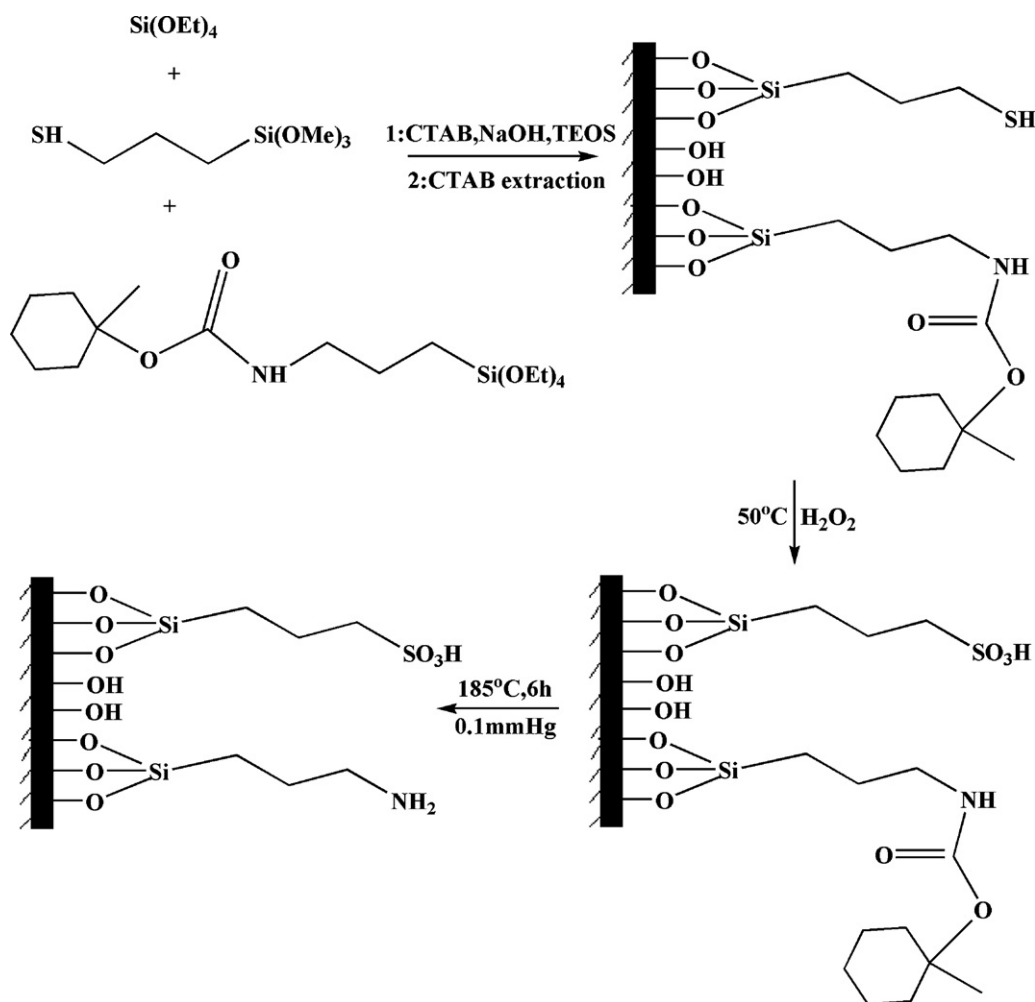
### 2.2. Chemical synthesis

#### 2.2.1. Synthesis of (3-triethoxysilylpropyl) carbamicacid-1-methylcyclohexylester (3TAME)

(3-Triethoxysilylpropyl) carbamicacid-1-methylcyclohexylester (3TAME) was prepared according to the modified literature procedure [24,25]. To a solution of 1-methylcyclohexanol (0.52 g) in 1,2-dichloroethane (15 mL), triethylamine (0.74 mL) and 3-(triethoxysilyl) propylisocyanate (1.03 mL) were added. The reaction mixture was stirred under N<sub>2</sub> for 24 h at 80 °C. The solvent was evaporated and the residue was denoted as (3-triethoxysilylpropyl) carbamicacid-1-methylcyclohexylester (3TAME).

#### 2.2.2. Synthesis of acid–base bifunctional materials

Synthesis of the bifunctional materials is shown in Scheme 1. Typically, 1.0 g cetyltrimethylammonium bromide (CTAB) was mixed with 240 g of distilled water and 7 mL 1.0 M NaOH solution. The premixed TEOS (5.2 mL), MPTMS (0.24 mL) and 3TAME (0.51 mL) were added into the above mixture after it was stirred for 30 min at 80 °C. The molar composition of the reaction mixture was (1–2x) TEOS:x 3TAME:x MPTMS:0.11 CTAB:0.28 NaOH:527 H<sub>2</sub>O (x = 0.05). The mixture was stirred for 2 h at 80 °C. The solution was filtered and the precipitate was washed with distilled water and then ethanol. The CTAB surfactant was extracted by stirring 1 g of the sample in a solution of 0.5 mL of HCl and 150 mL of ethanol for 5 h at 50 °C. The resulting mesoporous material was



Scheme 1. Synthesis of the bifunctional mesoporous materials of  $\text{SO}_3\text{H}$ -MCM-41- $\text{NH}_2$ .

filtered and washed with copious amount water and ethanol. The extracted material was then dried and denoted as SH-MCM-41-NHMch. The thiol groups were oxidized to sulfonic acid groups by  $\text{H}_2\text{O}_2$  in the presence of methanol for 24 h, and then stirred in a diluted sulfuric acid solution for 2 h [26–28]. The solid was washed with copious amount of water until a neutral pH, and dried overnight to obtain a dry white solid denoted as  $\text{SO}_3\text{H-MCM-41-NHMch}$ . The sample was then heated at  $185^\circ\text{C}$  for 6 h under vacuum to obtain the bifunctional mesoporous silica material containing aminopropyl groups and sulfonic acid groups, denoted as  $\text{SO}_3\text{H-MCM-41-NH}_2$ .

For comparison, mesoporous structural materials MCM-41- $\text{NH}_2$  (only use of 3TAME as organosiloxane), MCM-41- $\text{SO}_3\text{H}$  (only use of MPTMS as organosiloxane) and  $\text{HSO}_3\text{-M-41-NH}_2$  (use of MPTMS as organosiloxane, and use of APS substituting 3TAME) were prepared in a similar manner.

### 2.3. Characterization

Powder X-ray diffraction patterns (XRD) were collected using a Rigaku D/max-2200 ( $0.2^\circ/\text{min}$ ) with Cu  $\text{K}\alpha$  radiation (40 kV, 40 mA). Thermogravimetric (TG) analysis was carried out on a Shimadzu DTA-60 working in a  $\text{N}_2$  stream. The specific surface areas were obtained on a Micromeritics ASAP 2020 system at liquid  $\text{N}_2$  temperature ( $-196^\circ\text{C}$ ). Before measurements, the samples were outgassed at  $120^\circ\text{C}$  for 24 h. The specific surface areas were calculated by using the Brunauer–Emmett–Teller (BET) method and the pore size distributions were measured by using Barrett–Joyner–Halenda (BJH) analysis from the desorption branches of nitrogen isotherms. Transmission electron microscope (TEM) was performed on a Hitachi H-8100 electron microscope, operating at 200 kV.  $^1\text{H}$  NMR experiments were carried out in sealed NMR tubes on a Varian. The solid state  $^{13}\text{C}$  CP/MAS NMR using a Bruker AM-300 spectrometer with a frequency of 75.48 MHz. The solid state  $^{29}\text{Si}$  MAS NMR spectra were measured using a Varian Unity-400 spectrometer with 4 mm zirconia rotors spun at 4 kHz. Elemental analyses (EA) of N were performed on a VarioEL CHN elemental analyzer. X-ray photoelectron spectra (XPS) were recorded on a VG ESCA LAB MK-II X-ray electron spectrometer using Al  $\text{K}\alpha$  radiation (1486.6 eV). The measurement error of the spectra was  $\pm 0.2$  eV. A back titration method was used to measure the amount of acidic and basic centers of the materials according to the modified procedure in the literature [21,22]. About 0.1 g of the sample was added to a conical beaker, and then 10 mL 0.01 M HCl (NaOH) solution was added. The mixture was stirred at room temperature for half an hour; then, the mixture was filtered and rinsed repeatedly for four times with 25 mL distilled water. The resulting filtrate was titrated with 0.01 M NaOH (HCl) solution using phenolphthalein as indicator.

### 2.4. Catalytic tests

The aldol condensation reaction was performed in a flask under nitrogen [12,13]. First, 4-nitrobenzaldehyde (0.76 mg, 0.5 mmol) was dissolved in acetone (10 mL). Each catalytic reaction was carried out over 80 mg catalyst at  $50^\circ\text{C}$ . After the reaction, the product was filtered with acetone and chloroform to remove the solid catalyst. The resulting product was obtained and analyzed by  $^1\text{H}$  NMR in  $\text{CDCl}_3$ .

## 3. Results and discussion

### 3.1. Catalyst characterization

Fig. 1 shows the X-ray diffraction patterns of the prepared samples. All the materials exhibit a prominent peak of (1 0 0) and two weak peaks of (1 1 0) and (2 0 0) diffraction. The patterns were

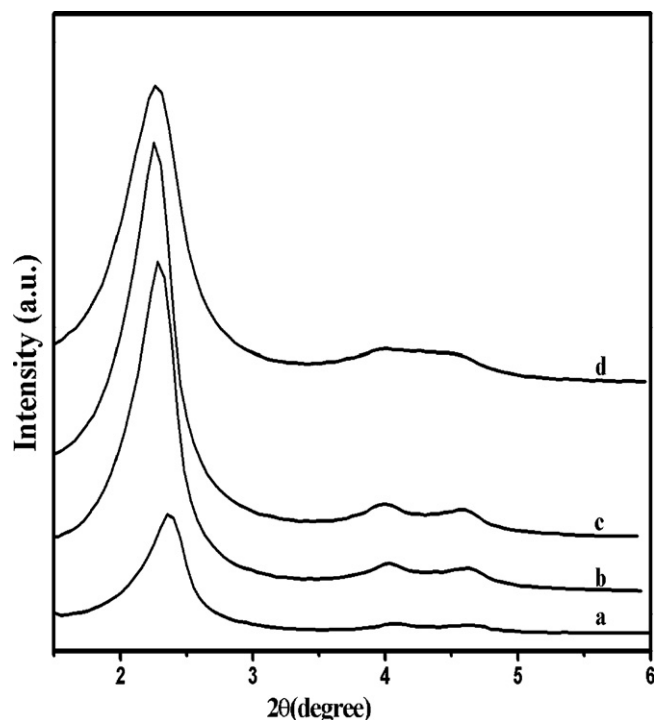


Fig. 1. Powder XRD patterns of (a) SH-MCM-41-NHMch (as-synthesized), (b) SH-MCM-41-NHMch (extracted), (c)  $\text{SO}_3\text{H-MCM-41-NHMch}$ , and (d)  $\text{SO}_3\text{H-MCM-41-NH}_2$ .

similar to that of pure siliceous MCM-41, indicating that the materials contain well-ordered hexagonal arrays. Although the crystallinity of the materials  $\text{SO}_3\text{H-MCM-41-NHMch}$  and  $\text{SO}_3\text{H-MCM-41-NH}_2$  decreases slightly, the similarity of the XRD patterns to pure siliceous MCM-41 indicates that the framework of  $\text{SO}_3\text{H-MCM-41-NHMch}$  and  $\text{SO}_3\text{H-MCM-41-NH}_2$  is still retained during the oxidation and thermolysis. TEM images of the synthesized samples are shown in Fig. 2. All the materials show well ordered and parallel pore structure. These results, together with the XRD patterns, confirm the formation of the highly ordered mesostructure.

The textural properties of the prepared samples are listed in Table 1. The total surface area gradually decreased from  $\text{SO}_3\text{H-MCM-41-NH}_2$  to SH-MCM-41-NHMch and  $\text{SO}_3\text{H-MCM-41-NHMch}$ . It is possible that organic groups in the material of  $\text{SO}_3\text{H-MCM-41-NHMch}$  are larger than other two samples. The pore diameter increases from 2.28 nm for  $\text{SO}_3\text{H-MCM-41-NHMch}$  to 2.38 nm for the sample of  $\text{SO}_3\text{H-MCM-41-NH}_2$ , and the pore volume increases from  $0.21\text{ cm}^3\text{ g}^{-1}$  for  $\text{SO}_3\text{H-MCM-41-NHMch}$  to  $0.28\text{ cm}^3\text{ g}^{-1}$  for  $\text{SO}_3\text{H-MCM-41-NH}_2$ . The results could ascribe to the decomposition of carbamate groups to amino groups in the process of thermolysis.

Quantification of the acidic and basic centers on the bifunctional mesoporous materials was performed using elemental analysis and back titration. The results of N elemental analysis in Table 1 indicate that there was 0.44 mmol/g of nitrogen for SH-MCM-41-NHMch, 0.41 mmol/g of nitrogen for  $\text{SO}_3\text{H-MCM-41-NHMch}$  and 0.46 mmol/g of nitrogen for  $\text{SO}_3\text{H-MCM-41-NH}_2$ . The results of the back titration are shown in Table 1. It is found that  $\text{SO}_3\text{H-MCM-41-NHMch}$  gives a loading of 0.39 mmol/g of  $-\text{SO}_3\text{H}$  and a small amount of loading of 0.008 mmol/g of  $-\text{NH}_2$ . However, after the thermolysis,  $\text{SO}_3\text{H-MCM-41-NH}_2$  gives a loading of 0.42 mmol/g of  $-\text{NH}_2$ , which are in good agreement with the loading of  $-\text{NH}_2$  obtained by elemental analysis results, further proving that the thermolysis of carbamate groups is an effective method to generate amines.

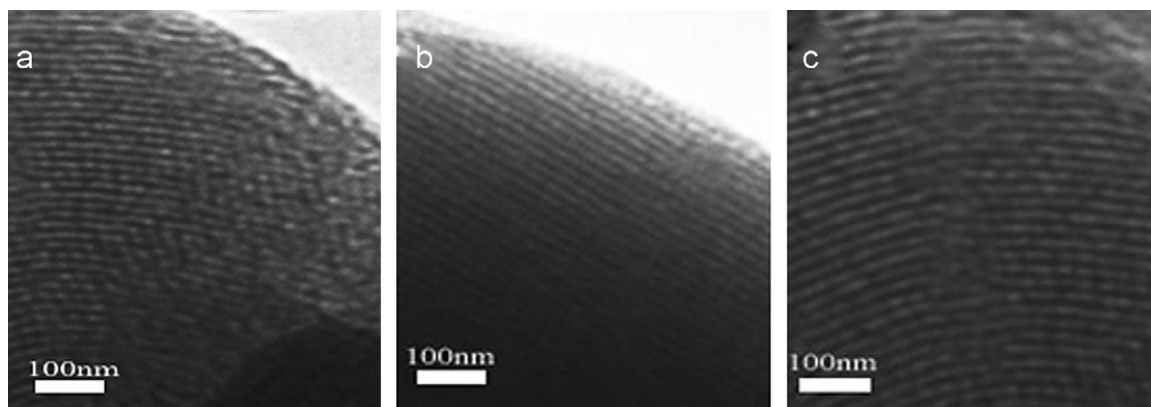


Fig. 2. TEM images of (a) SH-MCM-41-NHMch, (b) SO<sub>3</sub>H-MCM-41-NHMch, and (c) SO<sub>3</sub>H-MCM-41-NH<sub>2</sub>.

Table 1

The textural properties of the prepared materials.

Sample	$S_{\text{BET}}$ (m <sup>2</sup> g <sup>-1</sup> )	$D_p^a$ (nm)	$V_p$ (cm <sup>-3</sup> g <sup>-1</sup> )	N content <sup>b</sup> (mmol/g)	Acid amount <sup>c</sup> (mmol/g)	Base amount <sup>c</sup> (mmol/g)
SH-MCM-41-NHMch	793.8	2.37	0.22	0.44	–	–
SO <sub>3</sub> H-MCM-41-NHMch	734.8	2.28	0.21	0.41	0.39	0.008
SO <sub>3</sub> H-MCM-41-NH <sub>2</sub>	1017.9	2.38	0.28	0.46	0.41	0.42

<sup>a</sup> Calculated from desorption branch using the BJH method.

<sup>b</sup> Obtained from CHN elemental analysis.

<sup>c</sup> Obtained from back titration method.

Fig. 3 exhibits that the TG profiles of the prepared samples. Weight loss below 100 °C is due to the physically adsorbed water and ethanol inside the pores. The 4–5% weight loss at 100–200 °C is mainly related to the decomposition of surfactant template. The weight loss of 10% for MCM-41-NH<sub>2</sub>, 13% for SO<sub>3</sub>H-MCM-41-NH<sub>2</sub>, 15% for SH-MCM-41-NHMch, and 17% for SO<sub>3</sub>H-MCM-41-NHMch in the temperature range from 200 °C to 700 °C was mainly due to the decomposition of organic groups. Compare with SH-MCM-41-NHMch and SO<sub>3</sub>H-MCM-41-NH<sub>2</sub>, excess weight loss in SO<sub>3</sub>H-MCM-41-NHMch indicates that organic groups in the material of SO<sub>3</sub>H-MCM-41-NHMch are larger than other two samples.

The oxidation process was monitored by XPS. S2p core-level spectra of SH-MCM-41-NHMch and SO<sub>3</sub>H-MCM-41-NHMch are given in Fig. 4. Samples showed two types of sulfur species: one at low BE (163.7 eV), corresponding to a SH groups, and another at higher BE (168.6 eV), associated with sulfonic SO<sub>3</sub>H groups. Comparison between the spectra of the samples, only a peak appeared at 163.7 eV due to –SH groups in unoxidized sample SH-MCM-41-NHMch (Fig. 4a). This peak became weak and a new strong peak at higher BE (168.6 eV) associated with –SO<sub>3</sub>H groups was present after oxidation in Fig. 4b [29,30]. This result reveals that most of the precursor thiol (–SH) groups were oxidized to the sulfonic acid (–SO<sub>3</sub>H) groups by H<sub>2</sub>O<sub>2</sub> at 50 °C.

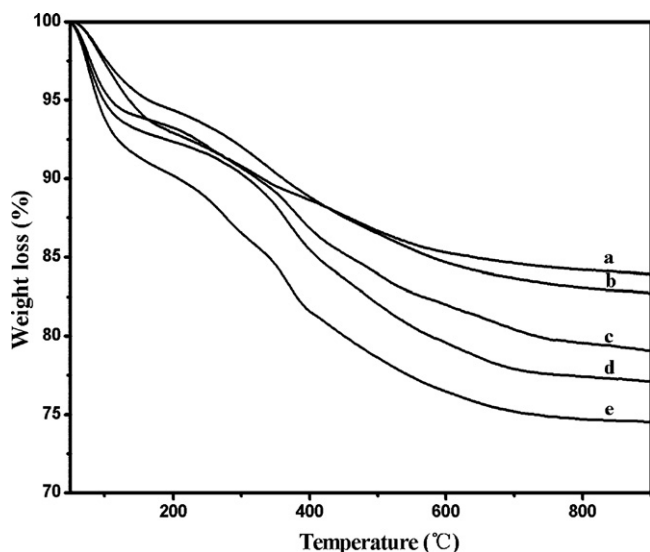


Fig. 3. TG profiles of (a) MCM-41, (b) MCM-41-NH<sub>2</sub>, (c) SO<sub>3</sub>H-MCM-41-NH<sub>2</sub>, (d) SH-MCM-41-NHMch, and (e) SO<sub>3</sub>H-MCM-41-NHMch.

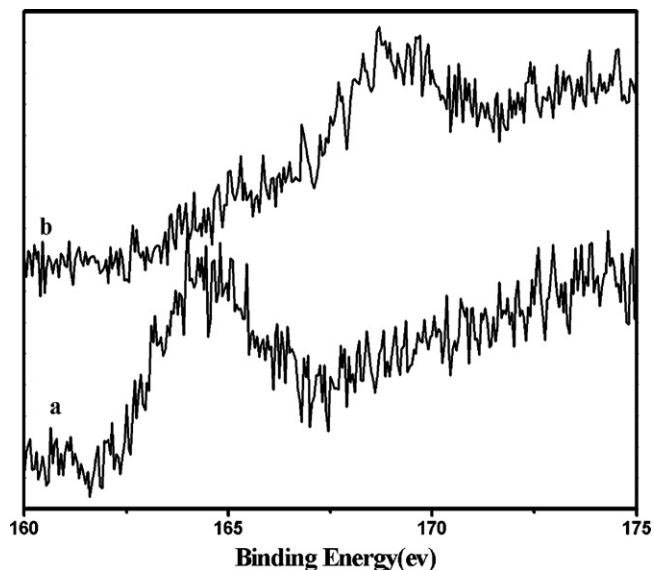


Fig. 4. S2p core-level spectra of (a) SH-MCM-41-NHMch and (b) SO<sub>3</sub>H-MCM-41-NHMch.

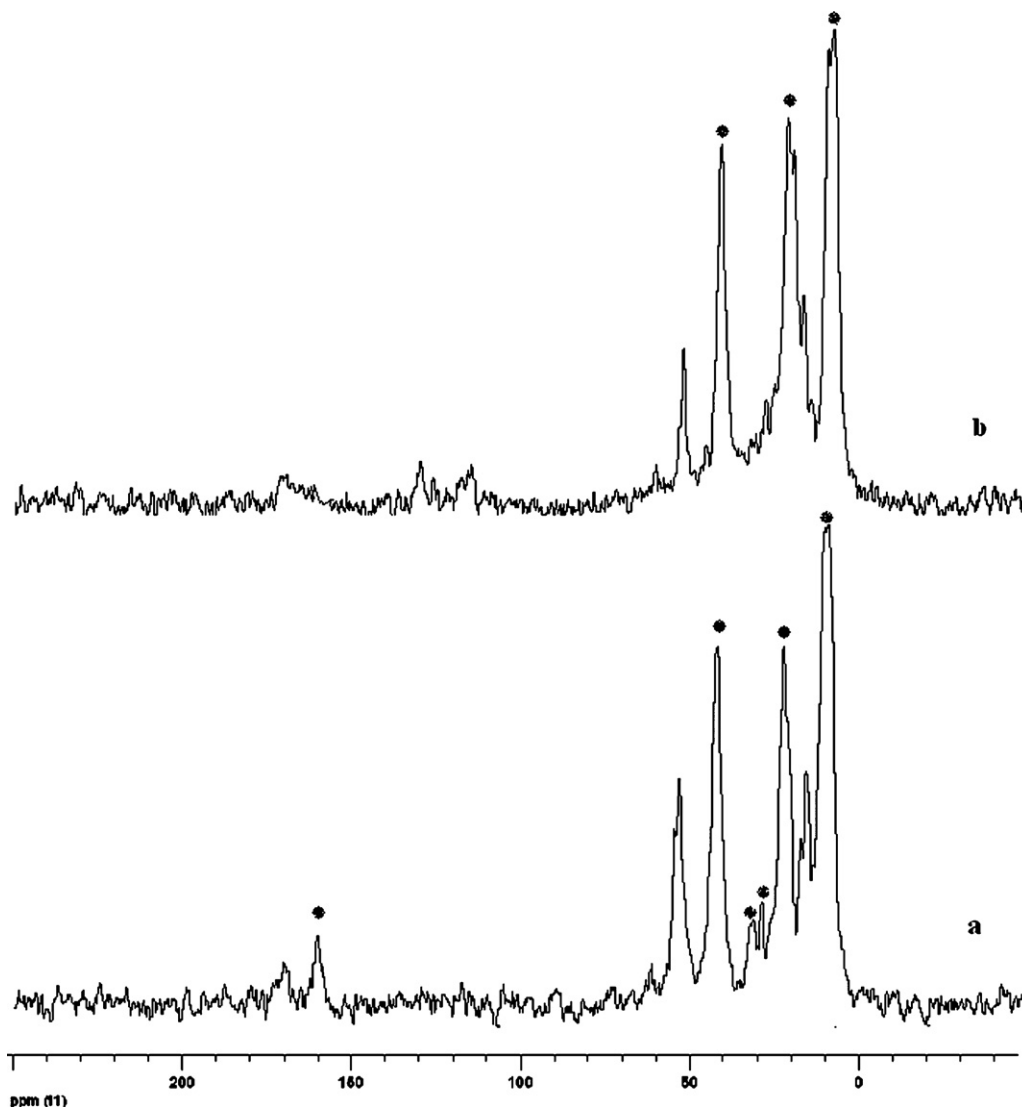


Fig. 5. Solid-state  $^{13}\text{C}$  CP/MAS NMR spectroscopy of (a)  $\text{SO}_3\text{H-MCM-41-NHMch}$  and (b)  $\text{SO}_3\text{H-MCM-41-NH}_2$ .

The successful incorporation of carbamate groups in the mesoporous materials and transformation of carbamate groups to the corresponding amino groups were confirmed by solid-state  $^{13}\text{C}$  CP/MAS NMR spectroscopy. The  $^{13}\text{C}$  CP/MAS NMR spectrum of  $\text{SO}_3\text{H-MCM-41-NHMch}$  is shown in Fig. 5a, the signals at 25.95 ppm ( $\text{CH}_3$  resonances), 32.25 ppm ( $\text{CH}_2$  of cyclohexyl) and 159 ppm (carbamate resonances) indicate that the methylcyclohexyl remained intact into the mesoporous MCM-41. The methylcyclohexyl was released by thermal treatment of  $\text{SO}_3\text{H-MCM-41-NHMch}$  at 185 °C for 6 h under vacuum. It is clearly reflected in Fig. 5b by the disappearance of resonances associated with the methylcyclohexyl and the carbamate group (25.95, 32.25 and 159 ppm), while the signals (7.85, 19.91 and 39.82 ppm) of the propyl spacer were retained [26]. It shows that methylcyclohexyl was released and carbamate group was successfully transformed into the corresponding amino groups by thermal treatment. These results are in good agreement with the conclusion drawn from TG analysis.

Solid-state  $^{29}\text{Si}$  MAS NMR spectroscopy has been proven to be the most useful technique for providing chemical information regarding the condensation of organosiloxane. As shown in Fig. 6, the peaks with chemical shift at  $-91.5$ ,  $-101.0$ , and  $-110.3$  ppm were attributed to the  $\text{Q}^2$ ,  $\text{Q}^3$ , and  $\text{Q}^4$  bands of  $\text{Si}(\text{OH})_2(\text{OSi})_2$ ,

$\text{Si}(\text{OH})(\text{OSi})_3$ , and  $\text{Si}(\text{OSi})_4$  silicate species, respectively. In addition, the resonance peak at  $-62.5$  ppm can be attributed to  $T^3$  ( $T^m = \text{RSi}(\text{OSi})_3(\text{OH})_{3-m}$ ,  $m = 1-3$ ), confirming that the organosiloxanes were condensed as a part of the silica framework [31].

### 3.2. Catalytic properties

The materials were used in the aldol condensation between acetone and various aldehydes (Table 2). The aldol condensation was reported to be catalyzed by acid, base and bifunctional acid–base catalysts. The reaction results show that pure silica MCM-41 almost gave no conversion of 4-nitrobenzaldehyde (entry 1). In the meanwhile, use of MCM-41 functionalized only with sulfonic acid groups gave relatively low conversion of 4-nitrobenzaldehyde (entry 2), while MCM-41 functionalized only with amino groups gave 85% conversion of 4-nitrobenzaldehyde (entry 3). In contrast, bifunctional catalyst material  $\text{SO}_3\text{H-MCM-41-NH}_2$  gave conversion to 95% (entry 7), illustrating that the acid–base cooperation effect should be involved in the catalytic reaction [12].

The superiority of acid–base bifunctional materials  $\text{SO}_3\text{H-MCM-41-NH}_2$  in catalytic behavior is also clearly reflected by the following results. Before the thermolysis to generate basic site,  $\text{SO}_3\text{H-MCM-41-NHMch}$  only gave conversion to 58% (entry 4).

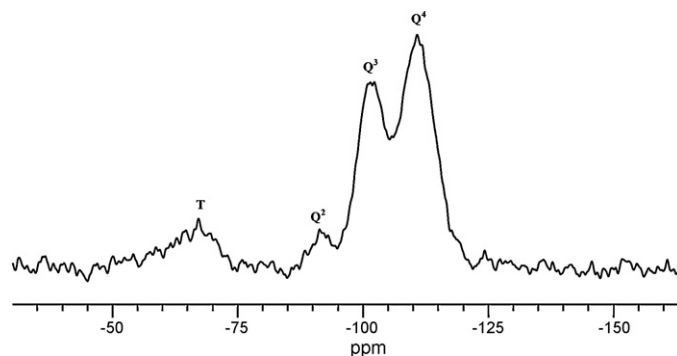
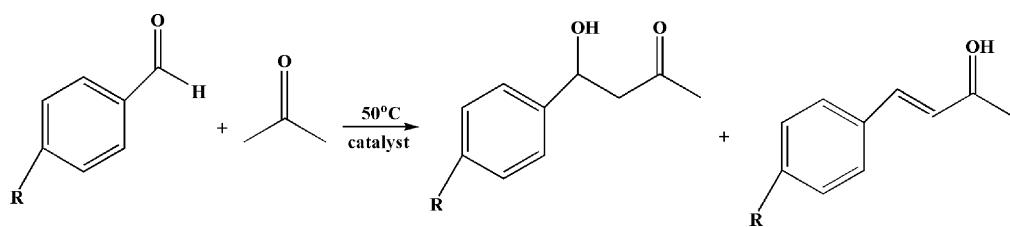


Fig. 6. Solid state  $^{29}\text{Si}$  MAS NMR spectroscopy of  $\text{SO}_3\text{H-MCM-41-NH}_2$ .

Table 2  
Test of catalysts



Entry	R	Catalyst <sup>a</sup>	A %	B %	Total conversion <sup>b</sup>	TOF <sup>d</sup> (h <sup>-1</sup> )
1	NO <sub>2</sub>	MCM-41	0	0	0	–
2	NO <sub>2</sub>	MCM-41-SO <sub>3</sub> H	12	6	18	–
3	NO <sub>2</sub>	MCM-41-NH <sub>2</sub>	78	7	85	–
4	NO <sub>2</sub>	SO <sub>3</sub> H-MCM-41-NHMch	53	5	58	–
5	NO <sub>2</sub>	SO <sub>3</sub> H-M-41-NH <sub>2</sub>	36	2	38	0.14
6	NO <sub>2</sub>	MCM-41-A/MCM-41-B <sup>c</sup>	50	4	54	–
7	NO <sub>2</sub>	SO <sub>3</sub> H-MCM-41-NH <sub>2</sub>	80	15	95	0.36
8	CF <sub>3</sub>	SO <sub>3</sub> H-MCM-41-NH <sub>2</sub>	79	14	93	0.35
9	CN	SO <sub>3</sub> H-MCM-41-NH <sub>2</sub>	78	8	86	0.32
10	H	SO <sub>3</sub> H-MCM-41-NH <sub>2</sub>	20	3	23	0.09

<sup>a</sup> 0.5 mmol aldehyde in 10 mL acetone stirred at 50 °C for 20 h.

<sup>b</sup> Total conversion determined through <sup>1</sup>H NMR spectroscopic analysis with THF as the internal standard.

<sup>c</sup> 1:1 mixture of sulfonic acid functionalized MCM-41 (MCM-41-SO<sub>3</sub>H) and amine-functionalized MCM-41 (MCM-41-NH<sub>2</sub>).

<sup>d</sup> TOF is based on mmol of aldehyde converted per mmol of active site.

However, when using bifunctional material  $\text{SO}_3\text{H-MCM-41-NH}_2$  as catalyst (entry 7), a significant improvement in conversion (to 95%) was observed. Meanwhile, a physical mixture of  $\text{MCM-41-NH}_2$  and  $\text{MCM-41-SO}_3\text{H}$ , showed a conversion that was obviously lower than  $\text{SO}_3\text{H-MCM-41-NH}_2$  (entries 6 and 7). These results further proved the bifunctional properties and the co-presence of acidic and basic active sites of  $\text{SO}_3\text{H-MCM-41-NH}_2$ . The performance of  $\text{SO}_3\text{H-MCM-41-NH}_2$  was not as good as  $\text{SO}_3\text{H-MCM-41-NH}_2$ , and it only gave 38% conversion of 4-nitrobenzaldehyde (entry 5), implying that a part of aminopropyl was oxidized by  $\text{H}_2\text{O}_2$  during the oxidation. The results confirm that thermolysis of carbamates to obtain the amino groups is an effective method to avoid oxidation of the amino groups. The thermolysis of carbamates to generate amino groups avoids either potential mutual destruction of acid–base groups or the protonation of the amino groups. Furthermore, the methylcyclohexyl can provide more steric hindrance to turn the acid–base distance. All these could be critical factors that make bifunctional material possess high activity for aldol condensation reaction. Also, the highest turnover frequency (TOF), expressed per mmol of aldehyde converted per mmol of active site, was achieved on the  $\text{SO}_3\text{H-MCM-41-NH}_2$ . It indicates that

the rate of per site was enhanced by the  $\text{SO}_3\text{H-MCM-41-NH}_2$ . The catalytic properties of synthetic materials have also been tested in aldol condensation reaction between acetone and other aldehydes with electron-withdrawing group (entries 8 and 9), and  $\text{SO}_3\text{H-MCM-41-NH}_2$  still exhibited higher conversion and TOF value. In addition, when without electron-withdrawing group is at position 4 (entry 10), poor conversion to the aldol product and TOF value is observed.

#### 4. Conclusion

In conclusion, a method for successful cohabitation of organic acids and organic amines on high-surface-area MCM-41 through oxidation and thermolysis is described. The novel method to obtain bifunctional material can reduce mutual destruction between sulfonic acids and amines and protonation of amino group. Furthermore, the methylcyclohexyl group can provide more steric hindrance to turn the acid–base distance. All these could be critical factors that make bifunctional material possess high activity for aldol condensation reaction. We also expect that the bifunctional materials can serve as novel selective catalysts for other important carbon–carbon bond forming reactions.

## Acknowledgments

The authors greatly appreciate the support of the National Natural Science Foundation of China (20673046) and Jilin Province (20090591).

## References

- [1] C.T. Kresge, M.E. Leonowicz, W.J. Roth, J.C. Vartuli, J.S. Beck, *Nature* 359 (1992) 710–712.
- [2] T. Yanagisawa, T. Shimizu, K. Kuroda, C. Kato, *Bull. Chem. Soc. Jpn.* 63 (1990) 988–992.
- [3] I. Rodriguez, S. Iborra, A. Corma, F. Rey, J.L. Jordá, *Chem. Commun.* 7 (1999) 593–594.
- [4] I.K. Mbaraka, D.R. Radu, V.S.Y. Lin, B.H. Shanks, *J. Catal.* 219 (2003) 329–336.
- [5] S.H. Shen, L.J. Guo, *Mater. Res. Bull.* 43 (2008) 437–446.
- [6] S. Dai, M.C. Burleigh, Y. Shin, C.C. Morrow, C.E. Barnes, Z. Xue, *Angew. Chem., Int. Ed.* 38 (1999) 1235–1239.
- [7] H. Yoshitake, T. Yokoi, T. Tatsumi, *Chem. Mater.* 15 (2003) 1713–1721.
- [8] V.S.Y. Lin, C.Y. Lai, J. Huang, S.A. Song, S.J. Xu, *J. Am. Chem. Soc.* 123 (2001) 11510–11511.
- [9] J.D. Bass, A. Solovyov, A.J. Pascall, A. Katz, *J. Am. Chem. Soc.* 128 (2006) 3737–3747.
- [10] F. Gelman, J. Blum, D. Avnir, *Angew. Chem., Int. Ed.* 40 (2001) 3647–3649.
- [11] S. Shylesh, A. Wagner, A. Seifert, S. Ernst, W.R. Thiel, *Chem. Eur. J.* 15 (2009) 7052–7062.
- [12] R.K. Zeidan, M.E. Davis, *J. Catal.* 247 (2007) 379–382.
- [13] R.K. Zeidan, S.J. Hwang, M.E. Davis, *Angew. Chem., Int. Ed.* 45 (2006) 6332–6335.
- [14] R.K. Zeidan, V. Dufaud, M.E. Davis, *J. Catal.* 239 (2006) 299–306.
- [15] C. Palomo, M. Oiarbide, J.M. García, *Chem. Soc. Rev.* 33 (2004) 65–75.
- [16] R.W. Snell, E. Combs, B.H. Shanks, *Top. Catal.* 53 (2010) 1248–1253.
- [17] S. Huh, H.T. Chen, J.W. Wiench, M. Pruski, V.S.Y. Lin, *J. Am. Chem. Soc.* 126 (2004) 11010–11011.
- [18] L. Beaudet, K.Z. Hossain, L. Mercier, *Chem. Mater.* 15 (2003) 327–334.
- [19] A. Walcarius, C. Delacote, *Chem. Mater.* 15 (2003) 4181–4192.
- [20] D.J. Macquarrie, D.B. Jackso, *Chem. Commun.* 18 (1997) 1781–1782.
- [21] Y.Q. Shao, J.Q. Guan, S.J. Wu, H. Liu, B. Liu, Q.B. Kan, *Micropor. Mesopor. Mater.* 128 (2010) 120–125.
- [22] J. Alauzun, A. Mehdi, C. Rey, R.J.P. Corriu, *J. Am. Chem. Soc.* 128 (2006) 8718–8719.
- [23] H. Li, S.T. Xu, W.P. Zhang, X.B. Lu, *Chin. Chem. Lett.* 20 (2009) 1051–1054.
- [24] E.G. Doyagüez, F. Calderón, F. Sánchez, A. Fernández-Mayoralas, *J. Org. Chem.* 72 (2007) 9353–9356.
- [25] J.D. Bass, A. Katz, *Chem. Mater.* 15 (2003) 2757–2763.
- [26] B. Râc, A. Molnr, P. Forgo, M. Mohai, I. Bertti, *J. Mol. Catal. A: Chem.* 244 (2006) 46–57.
- [27] E. Cano-Serrano, J.M. Campos-Martin, J.L.G. Fierro, *Chem. Commun.* 2 (2003) 246–247.
- [28] Q.Z. Wu, J.F. Liao, Q. Yin, Y.G. Li, *Mater. Res. Bull.* 43 (2008) 1209–1217.
- [29] R. Guo, X.C. Ma, C.L. Hu, Z.Y. Jiang, *Polymer* 48 (2007) 2939–2945.
- [30] E. Cano-Serrano, G. Blanco-Brieva, J.M. Campos-Martin, J.L.G. Fierro, *Langmuir* 19 (2003) 7621–7627.
- [31] X.S. Zhao, G.Q. Lu, *J. Phys. Chem. B* 102 (1998) 1556–1561.